Supporting Information

Salt Dissociation and Localized High-concentration Solvation by Interface of Fluorinated Gel and Polymer Solid Electrolyte

Dechao Zhang[1,2], Yuxuan Liu,[3] Dedi Li[1], Shimei Li[1,2], Qi Xiong[1,2], Zhaodong Huang[1,2], Shixun Wang[1], Hu Hong[1], Jiaxiong Zhu[1], Haiming Lv[2]*, Chunyi Zhi[1,2,4,5,6]*

[1] Hong Kong Center for Cerebro-Cardiovascular Health Engineering (COCHE), City University of Hong Kong, Shatin N. T. 999077, Hong Kong SAR, China

[2] Department of Materials Science and Engineering, City University of Hong Kong, Kowloon, 999077, Hong Kong SAR, China

[3]Guangdong Provincial Key Laboratory of Advanced Energy Storage Materials, School of Materials Science and Engineering, South China University of Technology, Guangzhou, 510641, China

[4]Hong Kong Institute for Advanced Study, City University of Hong Kong, Kowloon, Hong Kong, 999077, China

[5]Hong Kong Institute for Clean Energy, City University of Hong Kong, Kowloon 999077, Hong Kong

[6]Hong Kong Institute for Advanced Study, City University of Hong Kong, Kowloon, Hong Kong, 999077, China

*E-mail: haimilyu@cityu.edu.hk, cy.zhi@cityu.edu.hk

Methods

Materials

Poly(vinylidene fluoride-co-hexafluoropropylene) (PVDF-HFP, average Mw ~455,000), 2,2,3,4,4,4-hexafluorobutyl acrylate (HFBA, >95%), Azobisisobutyronitrile (AIBN, >99%), anhydrous N, N-dimethylformamide (DMF, >99.9) were purchased from Aladdin Biochemical Technology Co., Ltd. Fluoroethylene carbonate (FEC, >99.9%), Bis(2,2,2-trifluoroethyl) carbonate (TFEC, >99.9%), Bis(trifluoromethane)sulfonimide lithium salt (LiTFSI, ≥99.9%) were purchased from Dodochem without further purification. $LiFePO_4$ (LFP), and $LiNi_{0.8}Co_{0.1}Mn_{0.1}O_2$ (NCM811) powders, Super P, polyvinylidene fluoride (PVDF), Li foils (50 or 450 μm) were supplied by Canrd New Energy Technology Co., Ltd. (Dongguan, China).

Preparation of solid-state electrolytes

PVHF-HFP polymer matrix and LiTFSI salt were added into DMF solvent with a mass ratio of 1:0.6. The resulting homogenized slurry was then poured into a PTFE disk and dried in a vacuum oven at 120 °C for 12 h. The resulting polymer electrolyte membrane was labeled as PVHF-SPE. For the preparation of the fluorinated gel solid electrolyte (FG-SE), 0.1 wt% AIBN was dissolved in a nonaqueous mixture of TFEC: FEC: HFBA (6:3:1 by volume) with 1M LiTFSI to create a precursor solution. This solution was then heated at 70 °C for 3 h to yield a translucent gel, resulting in the FG-SE. To make the hybrid fluorinated gel and polymer solid electrolyte (HFGP-SE), the PVHF-SPE membrane was immersed into the fluorinated gel precursor solution for 3 h, then heated

at 70 °C for 3 h.

Characterizations

Fourier Transform infrared spectroscopy measurements were conducted using a PerkinElmer FTIR. Spectrometer X-ray photoelectron spectroscopy (XPS) spectra were conducted in a Thermo K-Alpha XPS spectrometer equipped with a monochromatic Al-Kα X-ray source. The micromorphology of products was analyzed by Field-emission scanning electron microscope (FESEM; Verios 5UC) and transmission electron microscopy (TEM) using an FEI Tecnai G2 f20 s-twin at 200kV. Raman spectra were obtained with a HORIBA JY LabRAM (532 nm). Thermogravimetry analysis measurements spanning 40 °C to 500 °C with a heat rate of 10 °C min^{-1} were performed under a N_2 atmosphere using a Q50 thermogravimetric analyzer. The molecular weight of poly (HFBA) is measured by gel permeation chromatography (GPC) with a Thermo Fisher Scientific MALLS-RI and the samples were dissolved in DMF.

All the electrochemical performances of the polymer electrolytes were measured by a CHI 760D electrochemical workstation. The ionic conductivity was determined through electrochemical impedance spectroscopy (EIS) employing a stainless steel (SS)||stainless steel (SS) coin cell. Measurements were conducted in the temperature range of 0 to 100 °C, with a frequency range from 1 MHz to 0.1 Hz and an AC amplitude of 10 mV. The ionic conductivity of the polymer electrolytes was calculated using the following equation:

$$\sigma = L/R \cdot S$$

where L is the thickness of the polymer electrolyte membrane, R is the bulk ohmic resistance, and *S* symbolizes the contact area between SS and the polymer electrolyte membrane.

The lithium-ion transference number (t_{Li^+}) of the polymer electrolyte was examined by combining AC impedance and DC polarization methods using a symmetrical Li cell. The value of t_{Li^+} is calculated according to the Bruce-Vincent-Evans equation:

$$t_{Li^+} = I_s\, Rb_s(\Delta V - I_0R_0)/I_0Rb_0(\Delta V - I_sR_s)$$

Where ΔV is the applied DC polarization voltage of 10 mV; I_0 and I_s present the direct current before and after polarization; and R_0 and R_s stand for the initial and final charge-transfer resistance of the polarization process; and Rb_0 and Rb_s are the initial and final resistances of the polymer electrolytes, respectively.

The electrochemical stabilities of the electrolytes were investigated through cyclic voltammetry (CV) and linear sweep voltammetry (LSV) measurements, measured on the SS||Li unsymmetrical cell at a scan rate of 1 mV s^{-1}. To evaluate the compatibility of electrolytes with Li metal, galvanostatic cycling measurements consisting of repeated 1h charge/discharge cycles were carried out in symmetrical Li||Li cells.

Assembly of battery and electrochemical measurements

The cathodes were prepared using a traditional slurry-coating method. In this process, cathode materials (LFP or NCM811), super P, and PVDF were wetly mixed in the NMP solvent with a weight ratio of 8:1:1. The resulting slurry mixture was cast onto a carbon-coated Al foil and dried at 80 °C for 8 h in a vacuum. The cathode was obtained with an active material mass loading of 2.5～3 mg cm^{-2}. The NCM811 cathode with a high

mass loading of 12 mg cm^{-2} was supplied by Canrd New Energy Technology Co., Ltd. (Dongguan, China). For the CR2032 type coin cell, the cathode was cut into disks of 10 mm diameter. For the pouch cells, cathode sheets of 4.6×5.4 cm^{-2} were selected to pair with 50 μm thick Li-Cu composite foil (Li-metal foil thickness of 50 μm on the Cu current collector). All the cells were assembled in an argon-filled glovebox with H_2O and $O_2 < 0.1$ ppm. The galvanostatic charge/discharge performances and electrochemical properties of the assembled cells were recorded by the LAND CT2001A testing system and CHI 760D electrochemical workstation, respectively.

Density functional theory (DFT) calculations

The DFT calculations were performed using the Gaussian16 program package with the B3LYP-D3 def2-TZVP basis set. Quantum chemical calculations of HOMO and LUMO energies were carried out using density functional theory.

The binding energy (E_b) between solvent and polymer molecules with Li salt was defined as follows:

$$E_b = E_{Li^+\text{-}TFSI^-\text{-}solvent} - E_{Li^+\text{-}TFSI^-} - E_{solvent}$$

where $E_{Li^+\text{-}TFSI^-\text{-}solvent}$, $E_{Li^+\text{-}TFSI^-}$, and $E_{solvent}$ represent the energy of the Li^+-$TFSI^-$-solvent cluster, Li^+-$TFSI^-$ salt and solvent, respectively.

Macromolecular Dynamic (MD) simulations

To simplify the calculation, 10 repeat segment units of $(\text{-}CH_2CF_2\text{-})_x[\text{-}CF_2CF(CF_3)\text{-}]_y$ (x: y = 3:1) represented the PVHF chains, and three repeat segment units represented the HFBA chains. The PVHF-SPE model was constructed based on the TGA-measured mass ratio of 57:33:10 for PVHF: LiTFSI: DMF (mass ratio). The FG-SE model was

constructed based on the ratio of TFEC: FEC: HFBA = 6:3:1 (volume) consisting of 1M LiTFSI. The simulation process included energy minimization with the steepest descent algorithm, followed by 5 ns NVT and 20 ns NPT simulations to ensure equilibrium. In the NPT process, the system was heated to 698.15 K and 1 bar for 2 ns, then cooled to 298.15 K for 3 ns and maintained at this temperature for 15 ns, followed by an additional 50 ns NPT simulation at 298.15 K and 1 bar. All simulations were conducted with a time step of 1 fs.

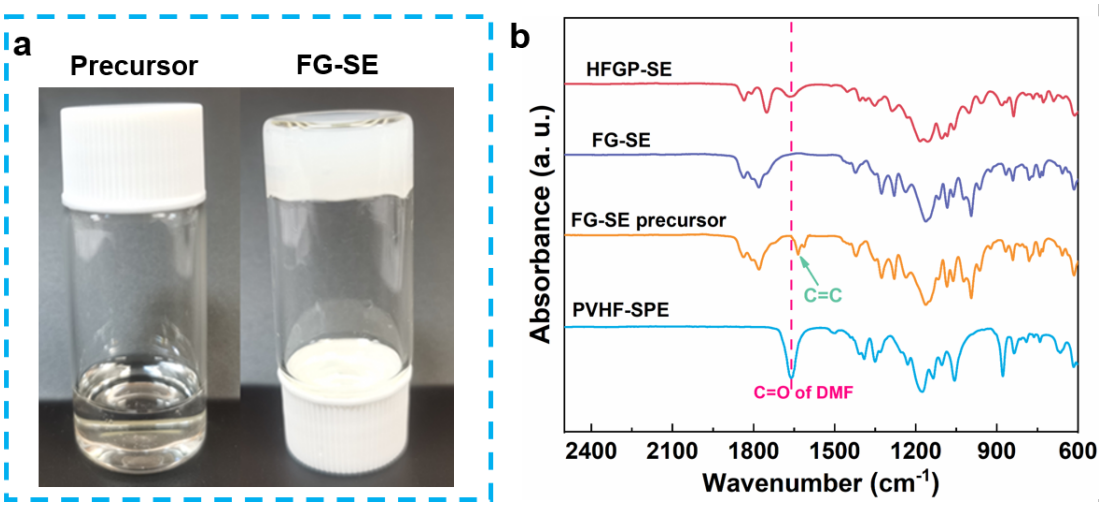

Figure S1. (a) Optical images of the FG-SE precursor solution and the corresponding FG-SE after polymerization. (b) FT-IR spectra of PVHF-SPE, FG-SE precursor, FG-SE and HFGP-SE.

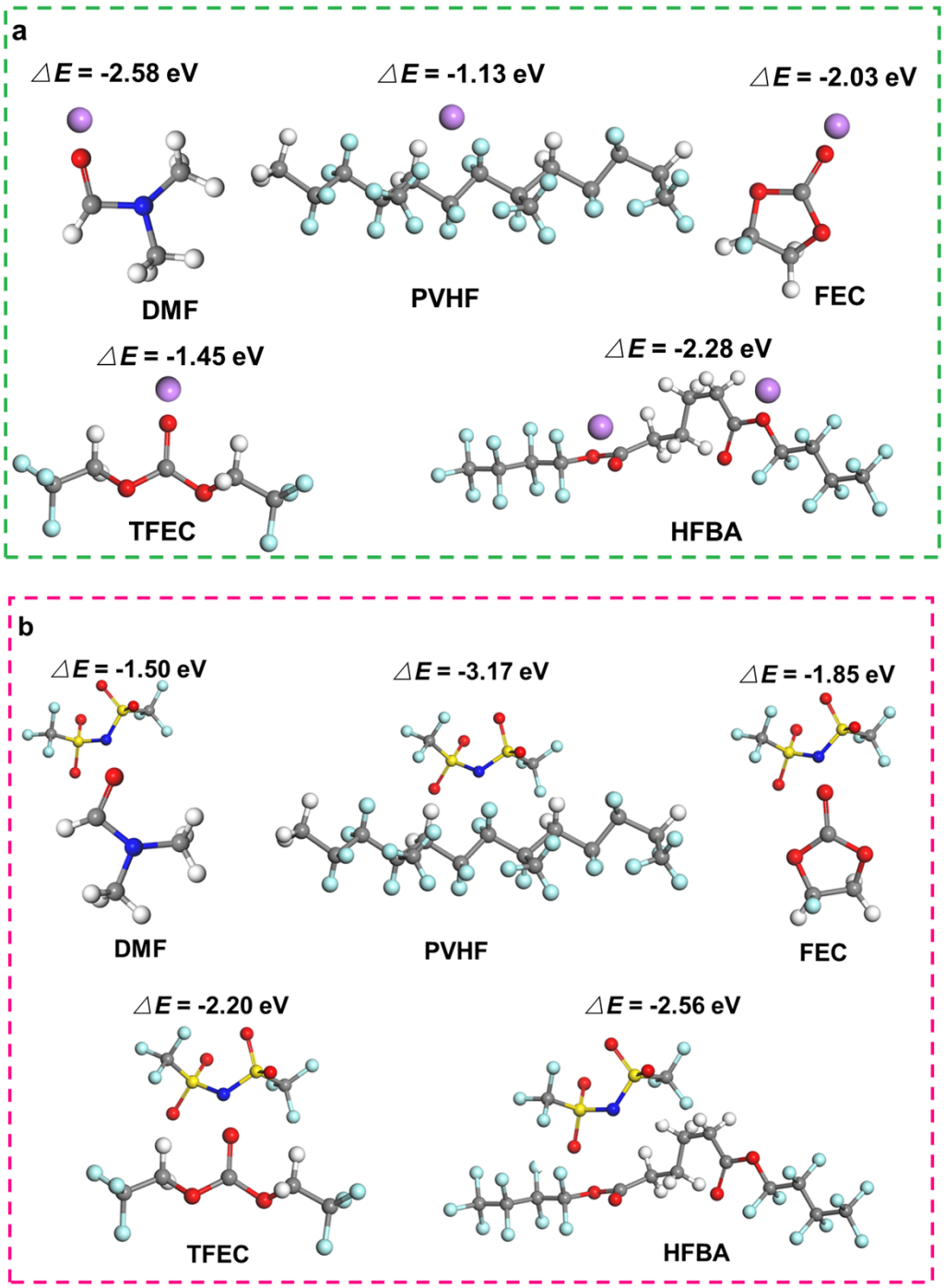

Figure S2. The molecular structures and corresponding binding energies of DMF, PVHF, FEC, TFEC, and HFBA for a Li^+ (a) and a $TFSI^-$ anion (b).

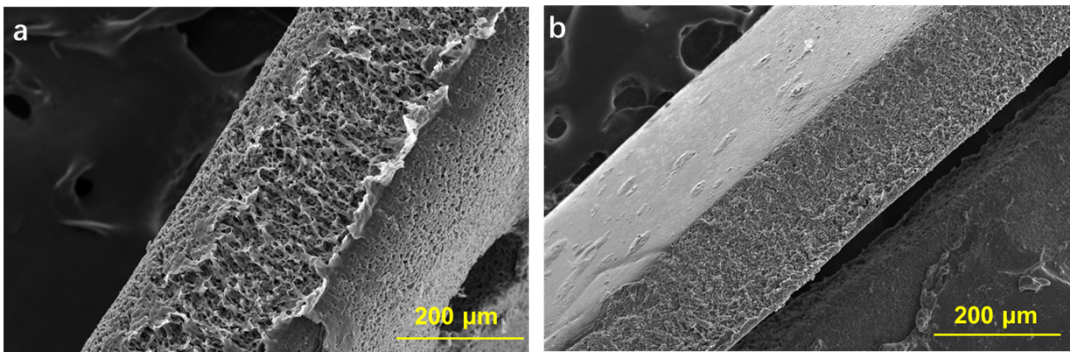

Figure S3. SEM image of the cross-section of (a) PVHF-SPE and (b) HFGP-SE.

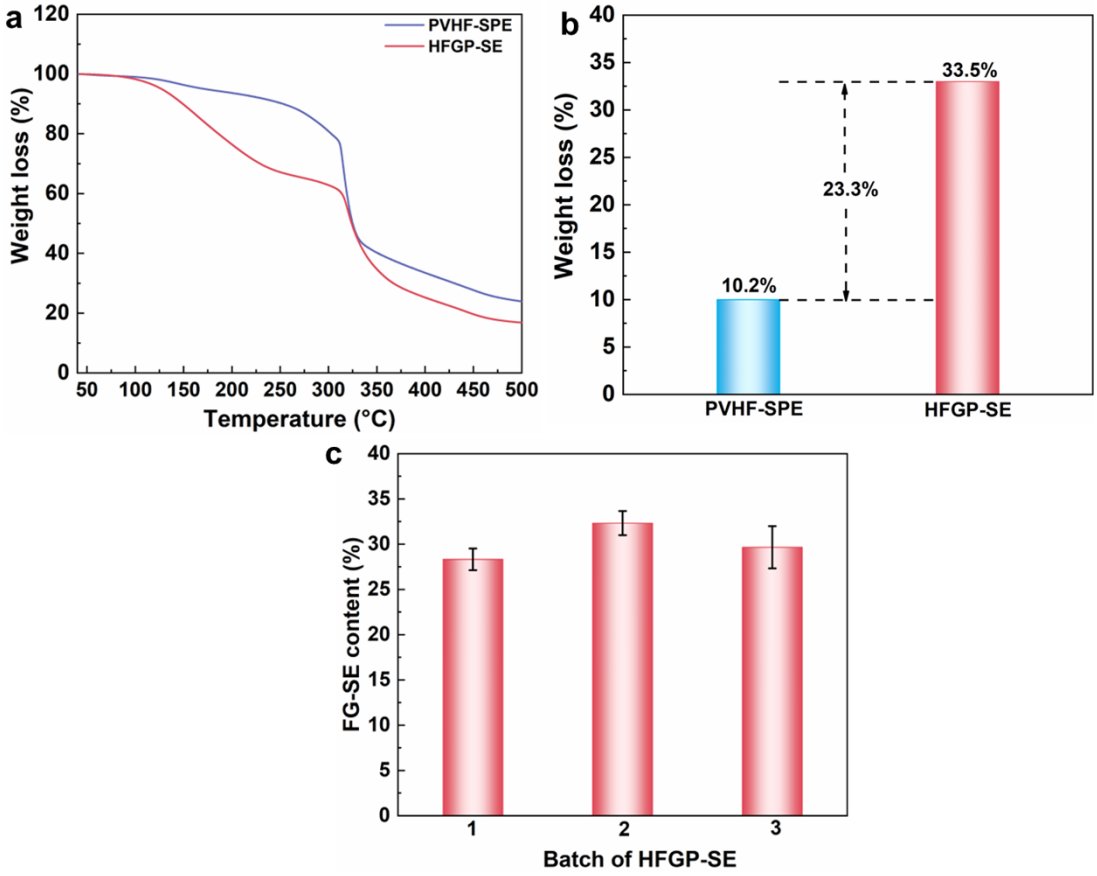

Figure S4. (a) TGA curves of PVHF-SPE and HFGP-SE. (b) The calculated liquid contents in PVHF-SPE and FG-SE contents in HFGP-SE. (c) FG-SE contents in HFGP-SE from different batches.

Note: The FG-SE contents ratio in HFGP-SE was calculated according the following equation:

FG-SE content (%) = $(W_1-W_0)/W_1$

where W_1 is the weight of HFPG-SE, W_0 is the weight of PVHF-SE.

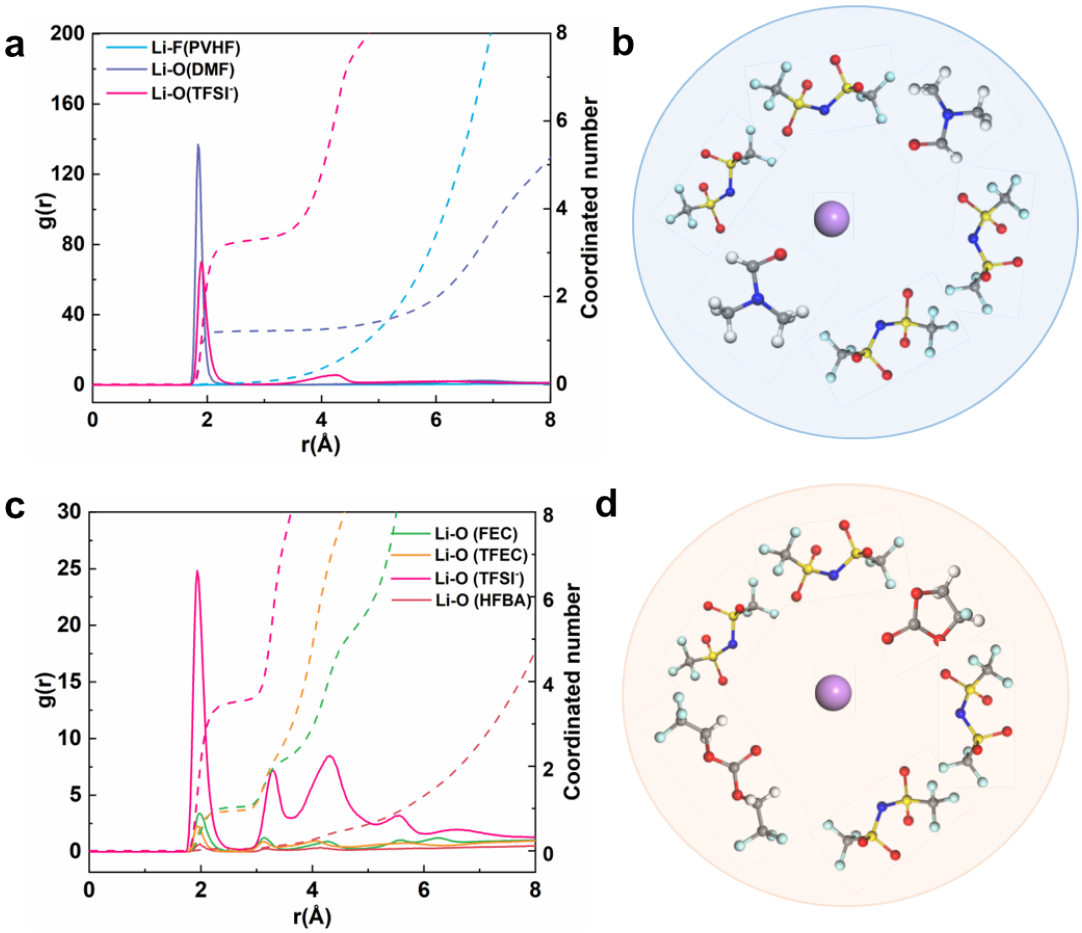

Figure S5. Radial distribution function (RDF), g(r), coordination number, and schematic diagram of the solvation structure of PVHF-SPE (a, b) and FG-SE (c, d).

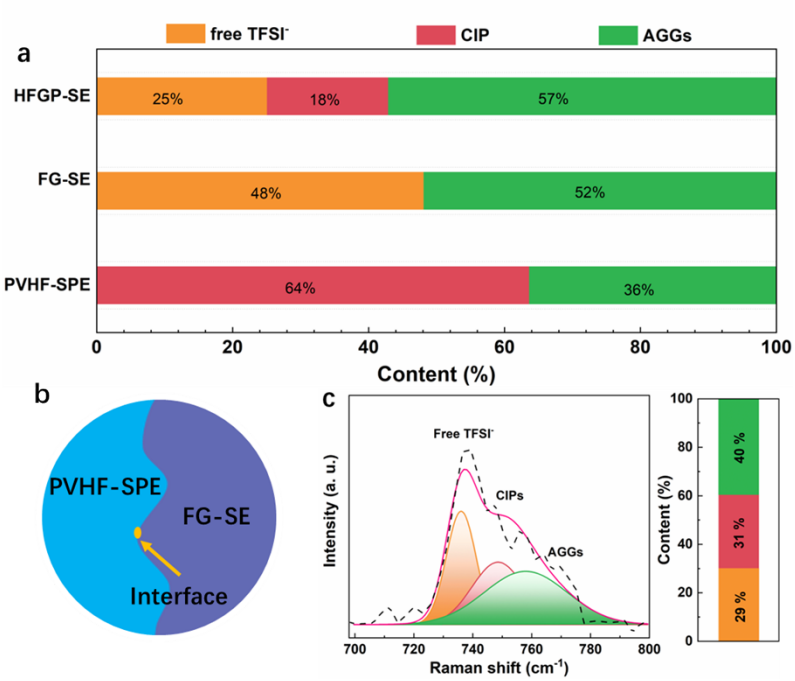

Figure S6. (a) The statistics on the ratio of different coordinates (free $TFSI^-$, CIP, AGGs), which are determined by the corresponding peak areas in Raman spectra. (b) (b) Schematic of the Raman detection area at the interface between PVHF-SPE and FG-SE, (c) Raman spectroscopy of the constructed interface between FE-SE and PVHF-SPE, and corresponding statistics on the ratio of different coordinates.

Note: To clarify the effects of the FG-SE and PVHF-SPE interface on the solvation structure, we constructed an electrolyte interface between FG-SE and PVHF-SPE and conducted Raman testing on the interfacial region (**Figure S6b, Supporting Information**). The Raman spectroscopy fitting results indicate that the interface contains 29 % free $TFSI^-$, 31 % CIP, and 40 % AGGs (**Figure S6b, Supporting Information**) . The higher ratio of free $TFSI^-$ and lower ratio of AGGs at the interface between FG-SE and PVHF-SPE (**Figure S6c, Supporting Information**) compared to that of HFGP-SE (**Figure S6a, Supporting Information**), indicates that the improved lithium salt dissociation at the interface between FG-SE and PVHF-SPE.

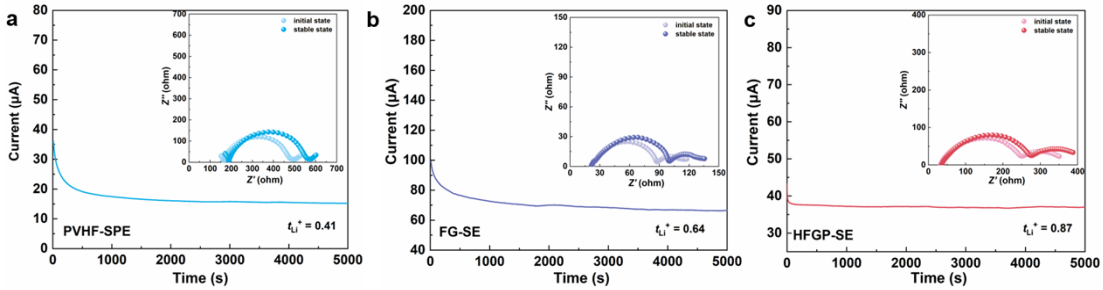

Figure S7. Polarization curves and the initial/steady-state electrochemical impedance spectroscopy of (a) Li||PVHF-SPE||Li cell, (b) Li||FG-SE||Li cell, and Li||HFGP-SE||Li cell.

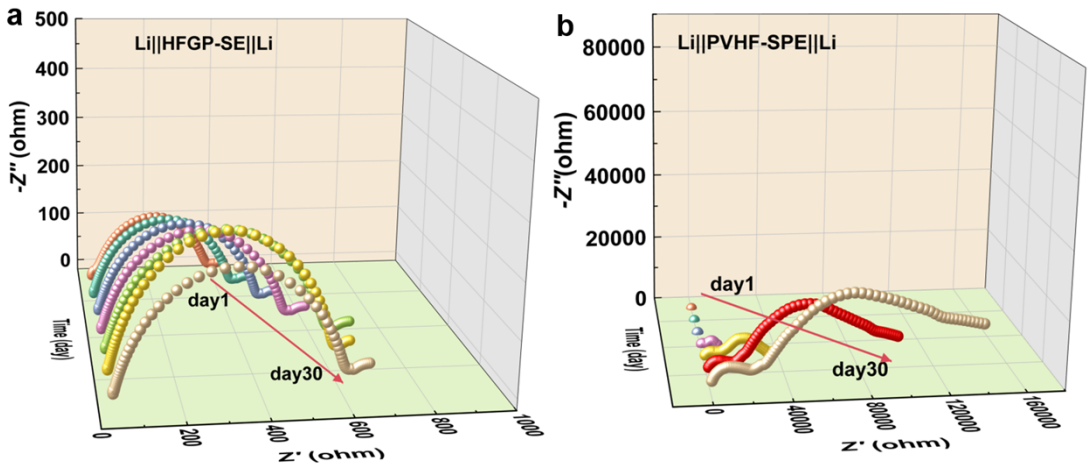

Figure S8. The time dependences electrochemical impedance spectroscopy (EIS) of (a) Li||HFGP-SE||Li and (b) Li||PVHF-SPE||Li cell.

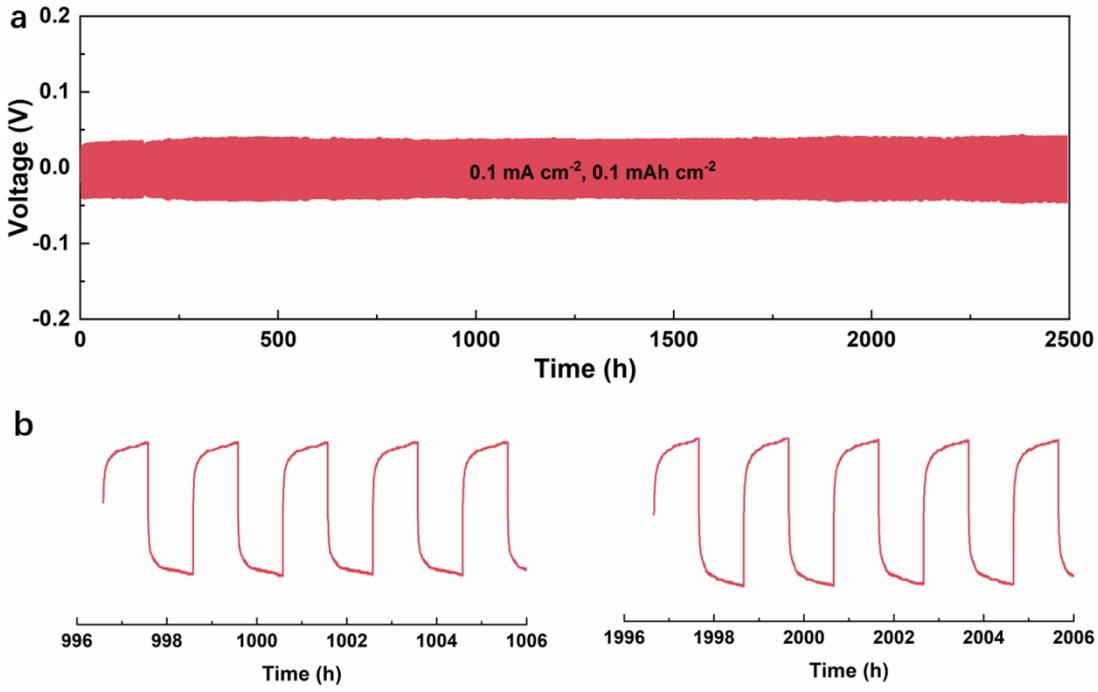

Figure S9. (a) Galvanostatic cycling curves of symmetrical Li||HFGP-SE||Li cell at current density of 0.1 mA cm^{-2}. (b) Locally amplified Voltage profiles of the Li||HFGP-SE||Li cell at different cycles.

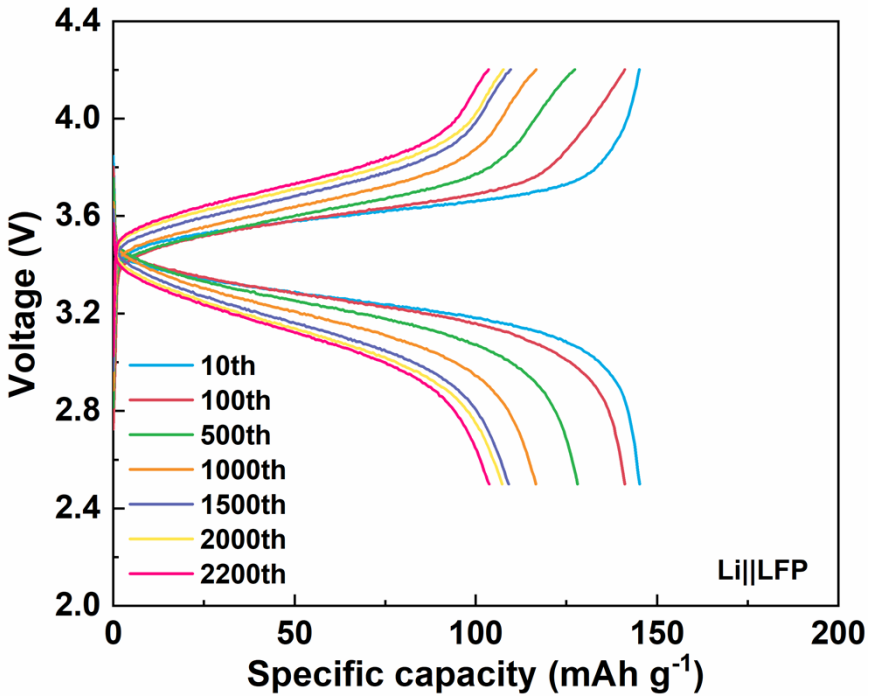

Figure S10. The charge/discharge profiles of Li||HFPG-SE||LFP after different cycles at 1C.

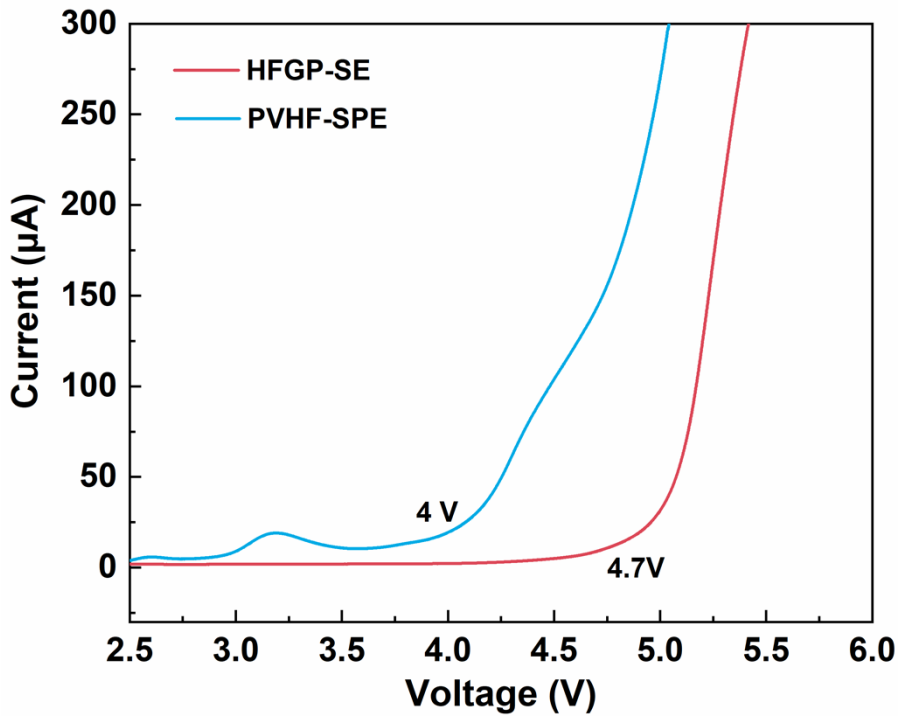

Figure S11. LSV curves of PVHF-SPE and HFGP-SE.

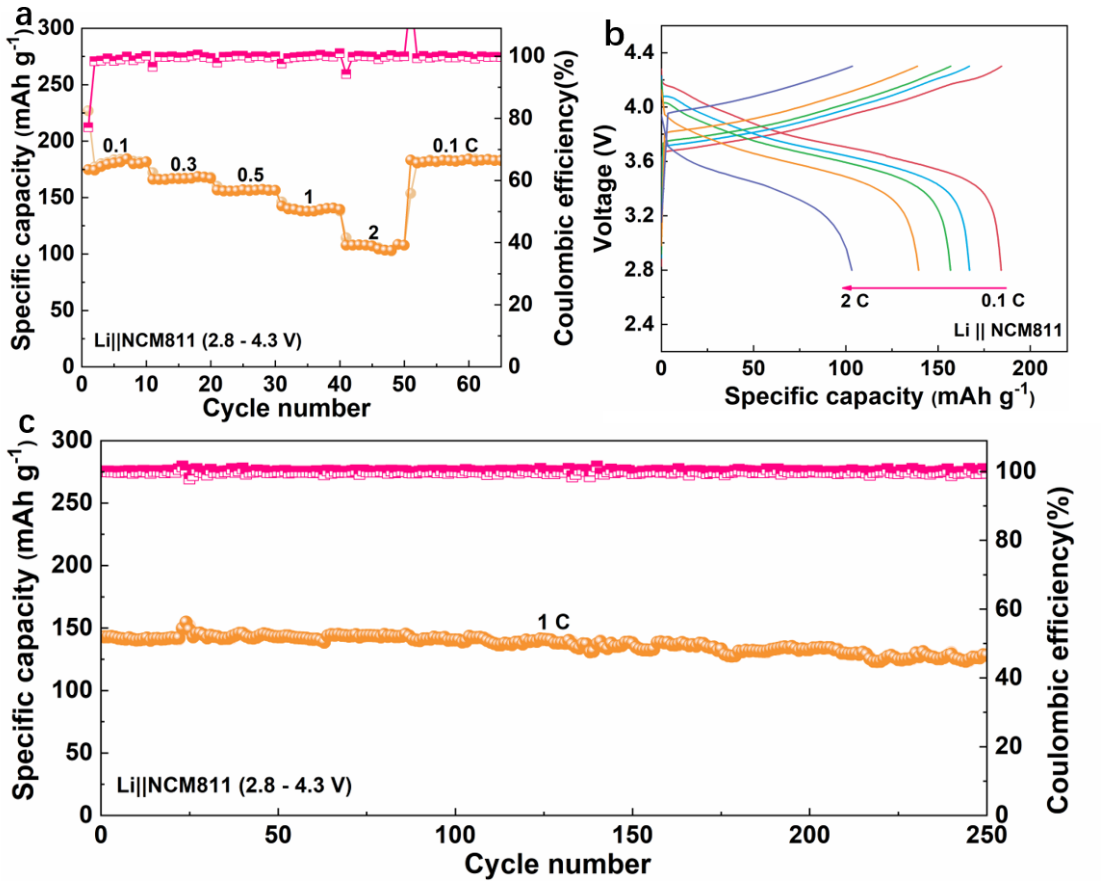

Figure S12. (a) Rate performance and **(b)** corresponding charge/discharge profiles of Li||HFGP-SE||NCM811 cell at the voltage range of 2.8 - 4.3 V. **(c)** Long cyclic performance of Li||HFGP-SE||NCM811 cell at 1 C.

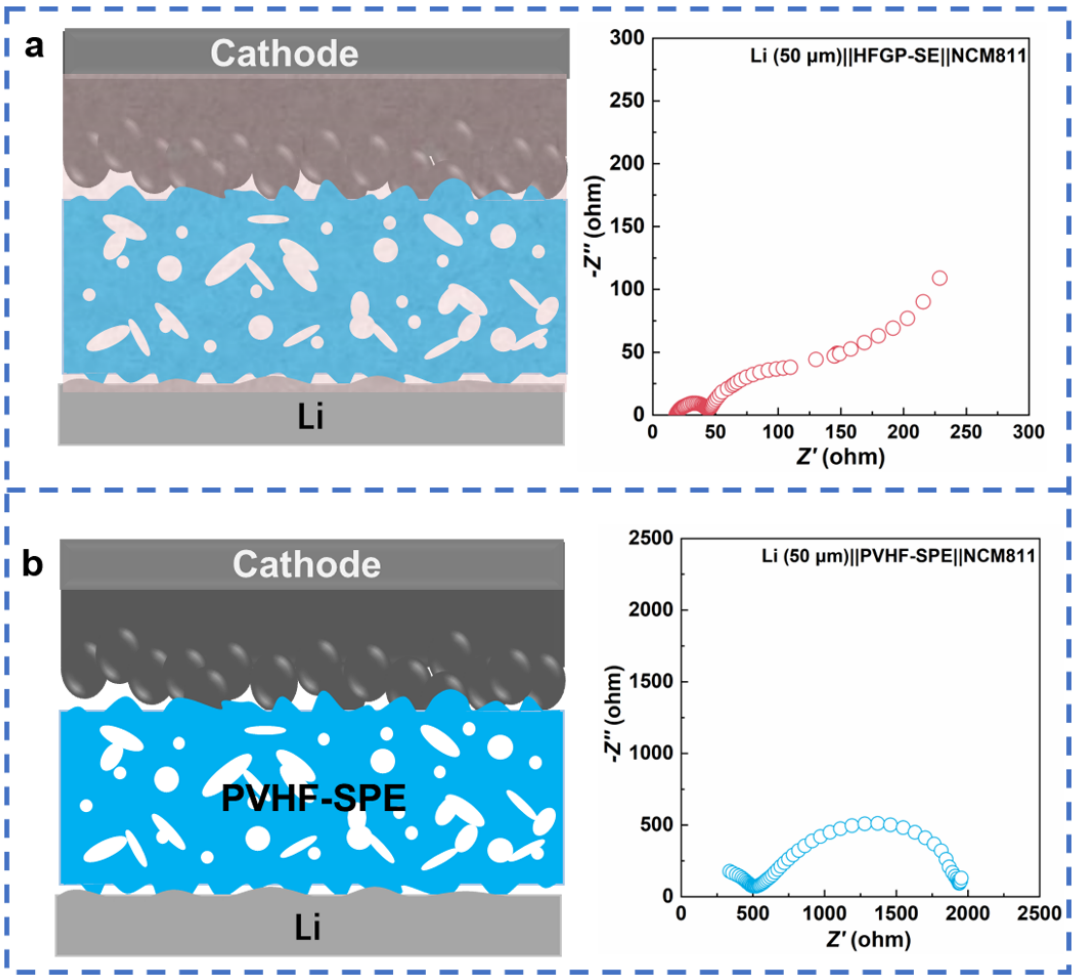

Figure S13. Schematic illustration and Electrochemical impedance spectroscopy (EIS) of Li (50 μm)||HFGP-SE||NCM811 cell (a) and Li (50 μm)||PVHF-SPE||NCM811 cell (b).

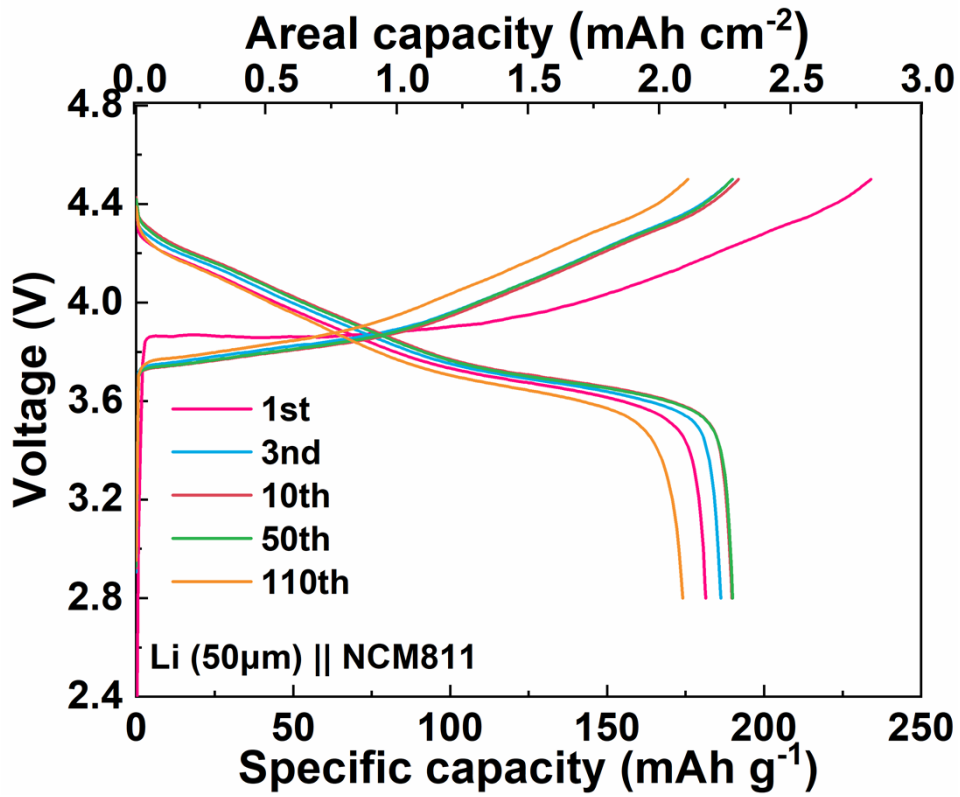

Figure S14. The charge/discharge voltage profiles of the coin cells with high-loading NCM811 cathodes (12 mg cm^{-2}) and 50 μm Li anode at 4.5 V cut-off voltage.

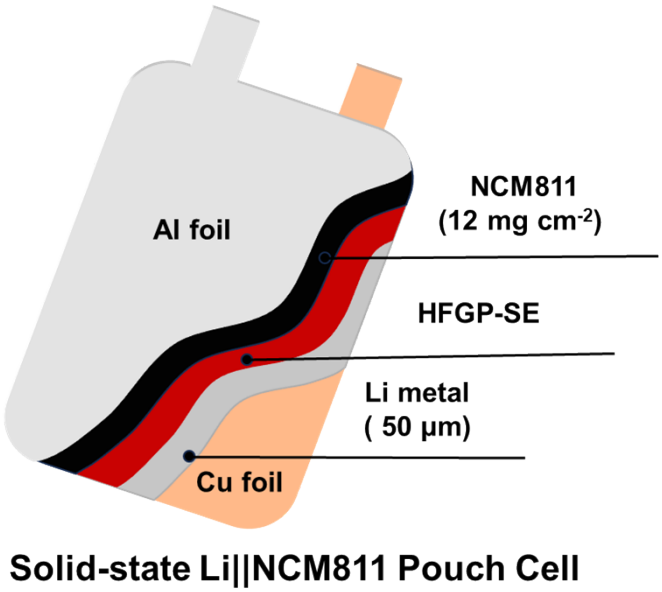

Figure S15. Schematic representation of the Li(50 μm)||HFGP-SE||NCM811 soft pouch type cell.

Supplementary Table 1. The molecular mass and polydispersity of poly(HFBA)

M_n	M_p	M_w	M_z	PD
138762	189665	144878	150448	1.044

Mn: the number average molecular weight

Mp: the peak molecular weight

Mw: the weight average molecular weight

Mz: the size average molecular weight

PD: polydispersity

Supplementary Table2. Comparison of the electrochemical performance of the solid-state lithium batteries in this work with that of other recently reported solid-state batteries using VDF-based SPEs.

Electrolytes	Main components	Cathode	Areal capacity (mAh cm^{-2})	Negative/Positive	Cut off voltage (V)	Ref.
PVT-10CuPcLi	PVDF-b-PTFE-lithiated copper polyphthalocyanine composite solid polymer electrolyte	NCM622	0.225	10	4.2	24
PVBL	poly(vinylidene difluoride)-$BaTiO_3$–$Li_{0.33}La_{0.56}TiO_{3-x}$ nanowires	NCM811	0.9	22	4.3	26
PVMS	poly(vinylidene fluoride)- MoSe2 sheets composite electrolyte	NCM811	1.44	6.9	4.3	27
TC-SPE	poly(vinylidene fluoride-trifluoroethylene-chlorotrifluoroethylene) (TerP)-poly(vinylidene fluoride-trifluoroethylene) (CoP) coupled SPE	NCM811	0.16	562	4.3	28
PVDF-GCN	g-C_3N_4 nanosheets (GCNs) reinforced poly(vinylidene fluoride) solid polymer electrolyte	NCM811	0.34	265	4.3	29
PVDF-LPPO	lithium phenyl phosphate (LPPO) grafted polyvinylidene difluoride (PVDF) based solid polymer electrolyte	NCM811	0.4	225	4.3	30

PVLN-15	**poly (vinylidene fluoride)-$Li_{1.4}Al_{0.4}Ti_{1.6}(PO_4)_3$ ceramic nanowires composite electrolyte**	**NCM811**	**0.67**	**134**	**4.3**	**31**
S-LHCE	**Polyvinylidene fluoride-hexafluoropropylene (PVDF-HFP)-dimethyl sulfoxide (DMSO) solidified localized high-concentration electrolyte**	**NCM811**	**0.32**	**281**	**4.3**	**32**
FPH-Li	**2D fluorinated graphene-reinforced PVDF-HFP-LiTFSI (FPH-Li) polymer electrolytes**	**NCM622**	**0.328**	**274**	**4.3**	**33**
PVDF-PZT	**poly(vinylidene fluoride) (PVDF)−$PbZr_xTi_{1-x}O_3$ (PZT) composite solid-state electrolytes**	**NCM811**	**0.15**	**600**	**4.3**	**34**
HFGP-SE	**hybrid fluorinated gel and polymer solid electrolyte (HFGP-SE)**	**NCM811**	**2.4**	**4.16**	**4.5**	**This work**